Journal of Agriculture and Environment Vol. 17 No. 1, 2021: 161-175
ISSN: 1595-465X (Print) 2695-236X (Online)

TEMPERATURE VARIABILITY AND IMPACT OF VEGETATION COVER IN IBADAN METROPOLIS, IBADAN, NIGERIA

U.J. Nwatu[1], A.A. Alo[1] and C.F. Agbor[2]

[1]Department of Social and Environmental Forestry, University of Ibadan, Ibadan, Nigeria
[2]Environmental Modeling and Biometrics, Forestry Research Institute of Nigeria, Jericho Ibadan, Nigeria

ABSTRACT

This study evaluates the changes in Urban Green Spaces (UGS) and the impact of such changes on surface temperature in Ibadan Metropolis between 1984 and 2018 using Landsat images. Digital numbers of the imageries were converted to physical quantities, radiance, and brightness temperature, while the temperature retrieval from thermal channels of Landsat imagery was carried out and the derived surface temperature validation was done through near-surface air temperature. This was followed by the reclassification of the images using Normalized Difference Vegetation Index (NDVI) as a proxy for vegetation cover and was regressed with urban temperature to observe their nexus, which explains the ability of UGS to absorb solar radiation in the study area. The land use land cover maps of the metropolis were developed from green, red and near-infrared channels of Landsat data in Idrisi software environment using maximum likelihood classifier. Results show that the mean temperature of Ibadan metropolis increased from 33.29℃ to 35.76℃ over 34 years, and the temperature of different land cover types considered in this study revealed that built-up and bare soil areas recorded the highest temperature changes compared to other land cover types (green spaces and water body). Also, the correlation analysis between UGS and ST showed a strong negative relationship with R^2 values ranging from -0.71 to -0.89. The study, therefore, concludes that the relationship is strong enough to ascertain that urban vegetation cover has the capacity to mitigate climate change effects. The increase in temperature may contribute to the variations in surface temperature, thus giving rise to the urban heat island effect. The study revealed the efficiency of geospatial techniques in data capturing for reliable information on sustainable management of urban green spaces.

Keywords: GIS; Urban green spaces; Urban heat island; surface temperature

INTRODUCTION

Urban green space (vegetation cover) contributes to the physiological, sociological, and economic well-being of urban society. Urban Green Spaces which vary in extent and distribution can be described as places in cities with significant amounts of vegetation

(Mwirigi *et al.*, 2012). A viable green space plays an important role in promoting the sustainable development of society because of the different ecosystem services it provides. Physical development in cities has affected the size of urban green spaces (Tang *et al.*., 2007). The green loss affects the microclimate condition of the city, which is capable of causing severe consequences on the environmental biotic cycle (Li *et al.*., 2016), due to the biophysical changes that modify the water cycle, surface energy balance, and alterations to the carbon balance (Li *et al.*, 2016).

According to Bakar (2016), variations in urban temperature can be explained by understanding the relationship between UGS and surface temperature (ST). Information on surface temperature can be used in a range of issues and themes in earth science such as global environmental changes and human-environment interaction (Hussain *et al.*, 2014), among others. Surface temperature is generally defined as the interface between the earth's surface and its atmosphere. (Qin and Karnieli, 1991; Khandelwa *et al.*, 2017). It is usually acquired directly from ground measurement, but these measurements cannot be generalized, as the surface temperature varied considerably from one surface type to another (Hussain *et al.*., 2014). ST can be retrieved from thermal images by the single infrared channel method or the split-window method, depending on the number of bands used. Remote sensing has been providing effective relevant information to better understand and monitor landscape development and processes, as well as estimate biophysical characteristics of land surfaces based on its advantage of repeatedly measuring a large spatial area (Roy *et al.*, 2001; Stow *et al.*, 2002; Tang *et al.*, 2007).

Geospatial technologies provide a seamless environment for integrating, visualizing, and analyzing digital data to facilitate change detection in a timely manner (Abed and Kaysi, 2003). Significant progress in the acquisition of remotely sensed data in a finer Spatio-temporal resolution, compounded with the development of geographic and environment process models, has greatly extended research capability to examine the changes in urban green spaces (Tang *et al.*, 2007). Hence, the relationship and spatial action of the objects in the geographical space can be well described via spatial analysis (Xiang and Han, 1997). Like many cities in developing countries, Ibadan has grown in population and territorial expansion, and this has led to changes in the extent and structure of green spaces (Raheem and Adeboyejo, 2016). Studies have in recent times observed that there is a relationship between vegetation loss and surface temperature changes in the tropics. According to past studies carried out using satellite surface temperature, the loss of vegetation cover results in significant temperature differences between green and non-green areas (Agbor *et al.*, 2018). These previous studies however did not emphasise what could be responsible for these observed relationships, which this research is set to achieve. To achieve this task, this study determined the urban green space distribution using NDVI, and the relationship between urban green space and surface temperature within the period under consideration in Ibadan metropolis.

MATERIALS AND METHOD

The Study Area

Ibadan metropolis is in Oyo State, Nigeria (Figure 1). It is the city at the junction of the savannah and the rain forest. It is the third-largest metropolitan area, by population, in Nigeria after Lagos and Kano, with a population of 2.84 million according to UN World

Urbanization Prospects (UNWUP, 2010). Ibadan city lies between latitude 7˚26'33"N and 7˚38'22"N and longitudes 3˚14'56"E and 3˚16'58"E (Agbor, 2012; Alo and Nwatu, 2018). The city is made up of 11 local government areas in which 5 forms the core urban area and the remaining 6 are classified as either rural or peri-urban local government areas (Popoola *et al..*, 2016). Ibadan is underlain by basement complex rocks which are mainly metamorphic rocks of pre-cambrian age with granite, quartzite and migmatite as the major rock types. The minor rock types include pegmatite, aplite, and diorite (Ajayi *et al.*, 2012). The soils of Ibadan region formed from the underlying rocks especially granite gneisse, quartz-schist, biotite, gneisses, and schist(Ajayi *et al..*, 2012). The climate of the city is a tropical climate with two distinct seasons. These are the rainy season, which spans through April to October and the dry season spanning through November to March. Temperature ranges between 25ºC and 35ºC (Agbelade *et al.*, 2016; Alo and Nwatu, 2018). The mean annual rainfall is above 1,505 mm while the relative humidity is between 60% and 80% (Raheem and Adeboyejo, 2016). The tropical forest exists in the south, while the guinea savannah predominates in the northern peripheries (Agbelade *et al.*, 2016). Ibadan lies mostly on lowlands which are punctuated by rocky outcrops and a series of hills. These outcrops are mainly granitic. Three major landforms of hills, plains, and river valleys dominate the whole landscape of the region. The average elevation is 230 m above sea level (asl). The metropolis is drained by three important rivers, R. Ogunpa, R. Ona and R. Ogbere and their several tributaries including Omi, Kudeti, Alaro and Alapata. This combination of hills and river valleys provide good drainage for the city (Ajayi *et al.*, 2012).

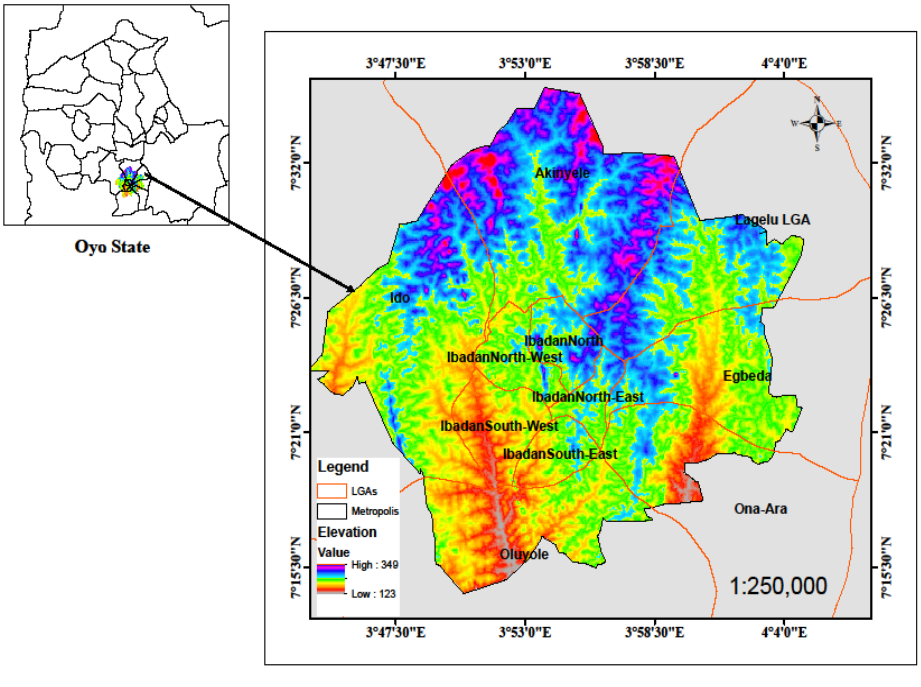

Figure 1: Ibadan metropolis, Nigeria.

Data Collection

This study involved two sets of data collection, which are primary and secondary data collection.

Primary data collection includes coordinates of some benchmark places with Ibadan metropolis, shapefile of the study area. The Secondary data collection includes Landsat satellite images of 1984, 2001 and 2018 (Table 1), the surface temperature of the study area (Table 2), and the digital elevation model (DEM) was downloaded from the official website of the US Geological Survey (USGS). This was used for land cover classification and temperature studies. Temperature value was obtained from ground weather stations and was used to validate temperature data obtained from satellite images. The study area is located in Landsat path 191 and row 55. The pixel sizes of the images are 30m x 30m (Chander, 2003). All the images were obtained in the same season (dry season).

Table 1: Satellite Images

Satellite Sensor	Spatial resolution	Acquisition Years	Path	Row	Source
Landsat 5, 7	30m x 30m	1984, 2001,	190	55	GLCF
Landsat 8 (OLI)	30m x 30m	2018	190	55	USGS

Table 2: Weather data

Weather data	Year	Source
Temperature from permanent stations	1984, 2001 and 2018.	Forest Research Institute of Nigeria (FRIN)

Data Processing and Analysis

Data Processing

Each pixel in unprocessed remote sensed data has a digital number value that corresponds to a raw measure required by the sensor (Giannini *et al.*., 2015). To obtain quantitative information from images, the digital number was converted to physical quantities, radiance and brightness temperature. It is necessary to correct images for atmospheric effects because the presence of the atmosphere can cause significant distortions in the radiometric signal. All images were resampled using resampling module in IDRISI environment to 30m x 30m. The land use land cover maps of the metropolis were developed from green, red and near-infrared channels of Landsat data in Idrisi software environment using maximum likelihood classifier. The images used in this study were first converted to Top of Atmosphere (TOA) radiance (equation 1) adopted from Giannini *et al.* (2015).

$$L\lambda = \left(\frac{(L_{MAX}\boldsymbol{\lambda} - L_{MIN}\boldsymbol{\lambda})}{Q_{CAL}\lambda}\right) Q_{CAL} + L_{MIN}\boldsymbol{\lambda} \qquad \ldots\ldots\ldots\ldots \qquad (eq.1)$$

Where:

Lλ =Spectral radiance at the sensor's aperture [W/(m^{2}sr µm)]

Q_{CAL} = Quantized calibrated pixel value [DN]

Q_{CAL}MIN = Minimum quantized calibrated pixel value corresponding to $L_{MIN}\lambda$ [DN]

$Q_{CAL}MAX$ = Maximum quantized calibrated pixel value corresponding to $L_{MAX}\lambda$ [DN]

$L_{MIN}\lambda$ = Spectral at-sensor radiance that is scaled to $Q_{CAL}MIN$ [W/(m²sr µm)]
LMAX, = Spectral at-sensor radiance that is scaled to Qcalmax [W/ (m 2 sr µm)].

The above expression does not consider the atmospheric effects, therefore there is a need to convert images from radiance to reflectance measures to remove the haze effect, using equation 2 by (Giannini *et al.*, 2015).

$$\rho\lambda = \frac{(\pi * \mathrm{TOAr.} * \mathrm{d}^2)}{E_{SUN}\lambda.\mathrm{Cos}\theta_{sz}} \quad \text{(eq.2)}$$

where;
$\rho\lambda$ = Planetary TOA reflectance (unitless)
π= mathematical constant approximately equal to 3.14159 (unitless)
$L\lambda$ = spectral radiance at the sensor's aperture [w/(m²sr µm)]
d^2 =the earth-Sun distance (Astronomical unit)
E_{SUN} =mean exoatmospheric solar irradiance [w/(m²sr µm)].
θ_{SZ}= the solar zenith angle (degree).

The cosine of this angle is equal to the sine of the sun elevation θ_{SE}. i.e.

$$\theta_{SZ} = \cos(90 - \theta_{SE}) \quad \text{(eq.3)}$$

These are rescaling factors given in metadata.

The grid referencing system of individual bands of each of the images used was transformed to one reference system (WGS_1984_UTM_Zone_31N). The re-projection is important to make an accurate analysis of the datasets and comparability possible.

Temperature Retrieval from Thermal Channels of Landsat Imagery

All the image bands are quantized as 8-bit data except Landsat 8 which is 16-bit, thus; all information was stored in DN which was converted to radiance with a linear equation (Giannini *et al.*, 2015) as given in equation 4.

$$L\lambda = MLQcal + Al \quad \text{(eq.4)}$$

Where:
$L\lambda$=TOAr (Top of Atmosphere) radiance - the radiance measured by the sensor
ML = Radiance multiplicative value
Qcal = Raw band
Al = Radiance additive value

By applying the inverse of the Planck function, thermal bands' radiance values were converted to a brightness temperature value using equation 5 (Giannini *et al.*, 2015).

$$B_t = \frac{K_2}{\left(\ln\left(\frac{k_1}{TOAr}+1\right)\right)} - 273.15 \quad \text{(eq.5)}$$

Where:

B_t= surface temperature
TOAr =Top of Atmosphere radiance
K_1 = calibration constant 1 (607.76 for TM), (666.09 for ETM+) and 774.89 for (OLI band 10)
K_2= calibration constant 2 (1260.56 for TM), (1282.71 for ETM+) and (1321.08 for OLI band 10)

Derived Surface Temperature Validation through Near-Surface Air Temperature

This method used the mean temperatures from three ground stations within the study area and the actual temperature in the given corresponding pixels on the same day of the satellite passing over the area for three representative points (Liu *et al.*, 2011).

The results of LST validation in quantitative form were evaluated using a bias equation (Schneider *et al.*, 2012):

$$Bias = LST\_sat - LST\_ref \quad \text{…….. (eq. 6)}$$

Where:
LST_sat = satellite-derived LST
LST_ref = observation of a given reference LST, which is assumed to be closer to the true value (Schneider et al., 2012).

This convention ensures that a positive bias is indicative of an overestimate of the satellite LST, whereas a negative bias reflects a satellite LST that is too low with respect to the reference data set. (Schneider *et al..*, 2012). Also, to visualise the deviations between the two measured parameters- LST from satellite and ground reference data, a regression line of all the matchups will be created. The reference surface temperatures (ground station data) will be plotted on the x-axis of the plot and the satellite-derived LST on the y-axis. This reveals the relationship between satellite-derived temperature and ground-based air temperature of three locations.

Relating Forest Cover with Temperature

To relate the forest cover with climate variable. NDVI has been used to assess the vigor of forest vegetation (Khan *et al..*, 2016). This index has been used to evaluate vegetation dynamics as it correlates with photosynthetic ability and net productivity (Ding *et al..*, 2007). It is stated as the difference between the near-infrared and red bands normalized by the sum of those bands (Nikolaos *et al.*, 2006). Equation 3 was used to create NDVI map.

$$NDVI = \frac{\rho NIR - \rho Red}{\rho NIR + \rho Red} \quad 3$$

Where:
ρNIR = near-infrared reflectance
ρRed = red reflectance

Determination of the Relationship between Urban Green Spaces and Surface Temperature

Correlation, also called correlation analysis, is a term used to denote the degree and direction of association or relationship between two (or more) quantitative variables

(Makinde *et al.*, 2019). This analysis is fundamentally based on the assumption of a straight–line (linear) relationship between the quantitative variables. Similar to the measures of association for binary variables. The result of correlation analysis is a *Correlation coefficient* whose *v*alues range from -1 to +1. A correlation coefficient of +1 indicates that the two variables are perfectly related in a positive (linear) manner, a correlation coefficient of -1 indicates that two variables are perfectly related in a negative (linear) manner, while a correlation coefficient of zero indicates that there is no linear relationship between the two variables being studied. The p-value at 0.05 was also used to assess the significance of the analysis. The correlation analysis of the pixel values of NDVI (urban green spaces) and LST was carried out in SPSS for the years considered in the study.*R* value was used to assess the relationship between UGS and LST. The coefficient of determination (r- squared) was that of Pearson correlation in equation 8.

$$r = \frac{N\sum xy - (\sum x)(\sum y)}{\sqrt{((N(\sum x^2) - \sum(x)^2)(N(\sum y^2) - \sum(y)^2))}} \qquad \ldots\ldots\ldots\ldots \qquad \text{(eqn. 8)}$$

Where:
N= number of pairs of scores
Σxy= sum of the products of paired scores
Σx= sum of x scores
Σy= sum of y scores
Σx^2 = sum of the squared x scores
Σy^2 = sum of the squared y scores
The comparison of land use land cover statistics over the years was handy in identifying the percentage change between 2013 and 2020 using equation 4 (Makinde *et al.*, 2018)

$$\%change = \left(\frac{c_x}{t_x} \times 100\right) - \left(\frac{c_y}{t_y} \times 100\right) \qquad 4$$

where c_x is the forest and non-forest cover for the base year, c_y stands for forest and non-forest cover for the later year, while t_x and t_y represent the total forest and non-forest cover for the base and later years respectively.

RESULTS

Spatial Distribution of Land Cover by NDVI

The spatial distribution of NDVI in Ibadan metropolis for 1984, 2001 and 2018 is shown in Figure 3. The highest NDVI value 0.39 was observed in 2018, followed by that of 1984, (0.37) and 2001 with 0.12 while the lowest value was observed in 1984, 2001and 2018 with the following values -0.28, -0.38 and 0.02, respectively.

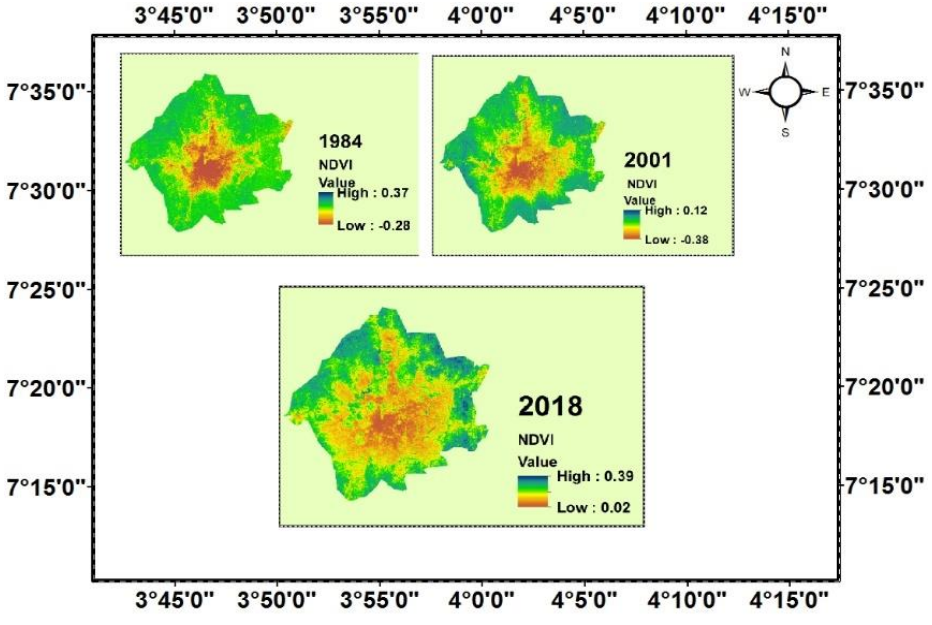

Figure 3: Normalized difference vegetation index of Ibadan metropolis

The NDVI images were reclassified into green space, built-up, water body, and bare soil (Figure 4).

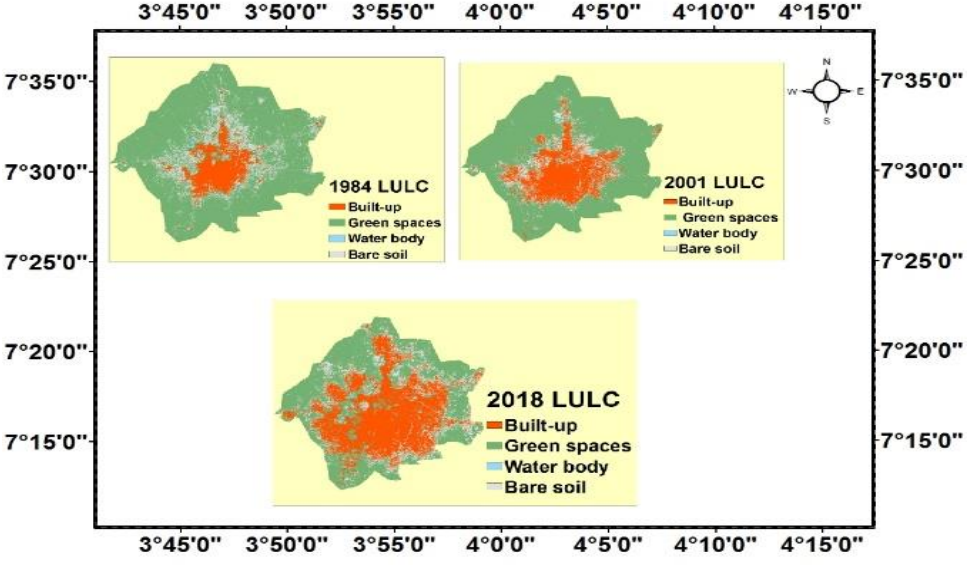

Figure 4: Land cover change types
Source*: Alo et al.* (2018)

In 1984, the green space occupied the largest area (126,344 ha) of Ibadan metropolis accounting for about 85.36% of the total area of the metropolis (Table 3). The built-up area, on the other hand, covered about 9,250.72 ha accounting for 6.25% and bare soil covered 12,193.00 ha accounting for 8.24% of the total land area, while the water body occupied the least area (233.01 ha) 0.16%. Between 1984 and 2001, the built-up area increased from 9,250.77ha accounting for 6.25% to 16,843.60 ha, which also accounted for 11.38% of the total land area. The urban green space land cover type recorded loss (126,344 ha describing (85.36%) to 122,838ha describing (82.99). In the same vein, water body land cover type decreased from 233.01ha accounting for 0.16% to 221.85 accounting for 0.15% and bare soil land cover type also decreased from 12,193 ha describing 8.23% to 8,117.28, describing 5.48% between 1985 and 2001. Going by the changes between 2001 and 2018, the built-up area recorded 10.39% increase (16,843.60 ha to 32,227.16 ha), bare land increased from 5.48% to 10.25% (8,117.28 ha to 15,176.20ha), while green spaces decreased by -15.11% (122,838 ha to 100,481.20 ha) and water body also decreased by -0.06% (221.85 ha to 136.17 ha) of the total area of Ibadan metropolis.

Table 3: Land use land cover between 1985 and 2017 in Ibadan metropolis

Classification	1985		2001		2017	
	Area (ha)	Area (%)	Area (ha)	Area (%)	Area (ha)	Area (%)
Green Spaces	126,344	85.36	122,838	82.99	100,481.20	67.88
Built-Up	9,250.72	6.25	16,843.60	11.38	32,227.16	21.77
Water Body	233.01	0.16	221.85	0.15	136.17	0.09
Bare Soil	12,193	8.23	8,117.28	5.48	15,176.20	10.25
Total	148,020.7	100	148,020.7	100	148,020.7	100

Source: Alo *et al.* (2018)

Assessment of Temperature Variations among the Different Land Cover Types

It was observed that built-up and bare-soil areas recorded the highest temperature in the study area with 29.25℃, 29.75℃ and 31.57℃ for built-up areas and 27.98℃, 28.82℃ and 32.97℃ for bare soil in 1984, 2001 and 2018, respectively (Table 4). The green spaces and water body, on the other hand, have the lowest temperature in the three years consistently with the following values 21.44℃, 22.33℃ and 23.04℃ for green spaces and 22.78℃, 19.21℃ and 22.51℃ for the water body in 1984, 2001 and 2018, respectively.

Table 4: Temperature variation in LC types of the study area

LULC	Temperature		
	1984 (℃)	2001 (℃)	2018 (℃)
Green spaces	21.44	22.33	23.04
Built-up	29.25	29.75	31.57
Water body	22.78	19.21	22.51
Bare soil	27.98	28.82	32.97

Validation of Temperature Values obtained from Satellite Imagery with Ground Data

The result in Table 5 showed a slight difference in the temperature obtained from satellite imagery when compared with that from the ground station. However, the estimate from the satellite images and ground observation exhibits a high level of correlation (0.89), which depicts a significant level of accuracy and relationship between both platforms.

Table 5: Temperature validation

Year	Satellite Temperature	Ground Station Temperature	Difference
1984	33.23	32.30	0.93
2001	34.01	33.50	0.51
2018	35.76	34.10	1.66

Source: Satellite imagery and ground station (FRIN), 2018

Relationship between Urban Green Spaces (UGS) and Surface Temperature (ST)

The spatial distribution of surface temperature over Ibadan metropolis is shown in Figure 5, the highest surface temperature (ST) of the study area (35.8℃) was recorded in 2018. This was followed by 34℃ in 2001 and 33.2℃ in 1984.

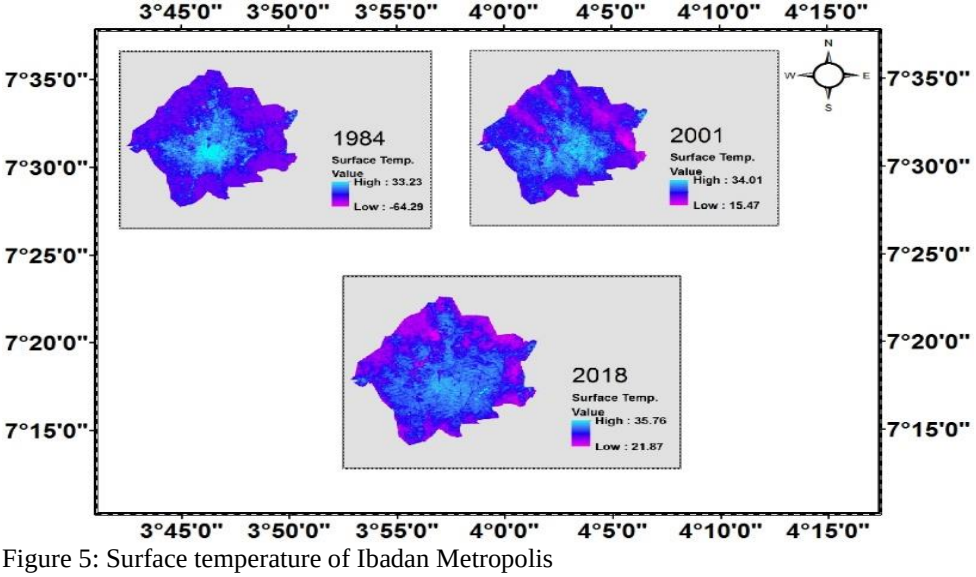

Figure 5: Surface temperature of Ibadan Metropolis

Tables 6 and 7 showed the correlation coefficients obtained from the correlation analysis between urban green spaces (NDVI) and surface temperature. One hundred sample points were randomly extracted from the temperature and NDVI images using Arc Toolbox in ArcGIS for the correlation analysis. Water features were excluded from the analysis. This was done due to the fact that studies have shown that surface temperature and NDVI have a negative correlation with water bodies, meaning that excluding such surfaces would increase

the accuracy of the correlation between surface temperature and NDVI values of the study area. The correlation coefficients of surface temperature and NDVI are -0.76, -0.71, and -0.89, respectively.

This showed that surface temperature (ST) and urban green spaces (UGS) have a negative correlation. The result was further validated using the p-values which were checked against the accuracy level of 0.05. The p-value is less than 0.05; hence, the result is reliable. The results can be used to explain the effect of green spaces on surface temperature increases over the years.

Table 6: NDVI and ST correlation result

	1984 NDVI	2000 NDVI	2017 NDVI	1984 Temp	2000 Temp	2017 Temp
1984 NDVI	1					
2000 NDVI	0.77	1				
2017 NDVI	0.54	0.71	1			
1984 Temperature	-0.76	-0.77	-0.56	1		
2000 Temperature	-0.55	-0.71	-0.61	0.78	1	
2017 Temperature	-0.47	-0.66	-0.89	0.61	0.71	1

Table 7: Correlation coefficient (r) and p- values

Year	Correlation coefficient value (r)	p-value
1984	-0.76	0.00
2000	-0.71	0.00
2017	-0.89	0.00

DISCUSSION

The range of ST from 33.25°C in 1984 to 35.75°C in 2018 depicting a consistent increase in the surface temperature could be attributed to an increase in human activities and the associated increase of accessibility to and within the forest reserve. This finding agrees with the report of Jibril (2010) that the rate at which the human population and its activities are increasing is alarming and a threat to the natural environment. Thus, affecting the natural ecology of the environment. Conversely, a decrease in forest cover over the years gives rise to a slight increase in temperature since there is a reduction in the amount of CO_2 trapped by the forest and consequently the release of O_2 during photosynthesis. Therefore, more CO_2 will be available to combine with other greenhouse gases and act like a blanket or a cap, trapping some of the heat that Earth might have otherwise radiated out into space leading to an increase in temperature (Florides and Christodoulides, 2009; Riphah, 2015; Weart, 2021).

The drastic loss of vegetation cover in the study area from 126,344 ha to 100,481 ha between 1984 and 2018 at the rate of -760.67 ha/yr. can be traced to the encroachment of city dwellers into urban forest areas and the dearth of proper urban forest management around and within the study area as observed during the field visit. Since the core of the metropolis is already congested with the population, there is a gradual movement of the people into the fringe of the metropolis thereby resulting in massive vegetation loss as one moves into the fringe of the metropolis (Rahman *et al..,* 2014; Wilcox *et al..,* 2017; Rahman *et al..,* 2017). This development is a potential ecological threat as such would alter the surface energy

balance with a consequent increase in land surface temperature within and outside the urban green space. This agrees with Pickett *et al.* (2001), Rahman *et al.* (2017), Zhou *et al.* (2019), that the removal of trees reduces the natural cooling effects of shading and evapotranspiration, thereby forcing the development of meteorological events such as increased temperature, which poses threat to the environment and the human population. Nowak *et al.*, (2002) related similar findings that forest lost intensifies air pollution, alter rainfall pattern in our environment, change the composition of biodiversity, and contributes to global warming.

The temperature increases by an average of 1.3ºC in a city suggests there is a global warming effect (Chen *et al.*, 2014; Zhou *et al.* 2019) otherwise, the temperature would not have increased by such value. This conclusion is based on the finding of Nastaran (2016), that tree planting is an efficient method to mitigate the heat island effect and human health consequences of increased temperatures resulting from climate change. This phenomenon is described as an urban heat island (UHI). The thermal comfort of city inhabitants is directly (Lafortezza *et al.*, 2009) and indirectly (Stafozzia *et al.*, 2008) affected by UHIs. UHIs not only influence water use and biodiversity change but also contribute to human discomfort by increasing the cause of mortality and disease (Basara *et al.*, 2010) and at the same time increase the heat budget of the city.

The strong negative correlation coefficient between temperature and NDVI indicates that the impact of green land on temperature is negative, which means that the green land can weaken the urban heat effect. It also shows that the vegetation within the metropolis is capable of absorbing solar energy used up by the vegetation terrain thereby reduces energy available to heat up the environment. The estimate from the satellite images and ground observation in figure 4 exhibited a slight difference in their values, although with a high level of correlation (0.89). The observed slight difference might be caused by the radiometric error of the satellite platform and variation in the time of the day both data were taken.

CONCLUSION

Vegetation plays a crucial role in sustaining the natural environment and humanity. This study examined the effect of vegetation loss on temperature variability as a component of climate change using satellite data. Findings show that green space reduced and developed areas increased in 2018. The reduction in urban green space was attributed to the quest for forest products such as wood for construction, clearing of the forest for agriculture, illegal logging and gathering of fuelwood. Results from the correlation analysis show negative relationships between UGS (NDVI) and urban temperature. Though the relationships are strong enough for this study to conclude that the UGS has the capacity to mitigate climate change effects with a high ability to absorb radiation, further research should consider the surrounding settlements and environment before a generalization can be made. Relevant authorities should put measures in place to reduce UGS loss and the adverse effects of such development.

REFERENCES

Abed, J. and Kaysi, I. (2003). Identifying urban boundaries: application of remote sensing and geographic information system technologies. *Canadian Journal of Civil Engineering*, 30: 992—999.

Agbelade, J., Aladesanmi, D., Onyekwelu, J.C. and Apogbona, O. (2016). Assessment of urban forest tree species population and diversity in Ibadan, Nigeria. *Environment and Ecology Research*, 4, 185 - 192.

Agbor, C.F. and Makinde, E.O. (2018): Land Surface Temperature Mapping Using Geo-information Techniques, *FCE CTU* 17(1),

Agbor, C.F., Aigbokhan, O.J., Osudiala, C.S., Malizu, L. (2012). Land use land cover change prediction of Ibadan metropolis. *Journal of Forestry Research and Management*, 9, 1-13

Ajayi, O., Wahab, B., Gbadegesin, M., Taiwo, D., Kolawole, O., Muili, A., Shiji, F. (2012). Flood Management in an Urban Setting : A Case Study of Ibadan Metropolis. *Hydrology for Disaster Management*. A special Edition. 65–81.

Alo, A. A., and Nwatu, J. U. (2018). Modeling urban green space dynamics and associated proximate drivers in Ibadan metropolis, Ibadan, Nigeria. *Forests and Forest Products Journal,* 18: 23-34

Bakar, S.A., Pradhan, B., Lay, U.S., Abdullahi, S. (2016). Spatial assessment of land surface temperature and land use/land cover in Langkawi Island**,** 8th IGRSM International Conference and Exhibition on Remote Sensing & GIS (IGRSM 2016) *Earth and Environmental Science*, 37 (2016) 012064 doi:10.1088/1755-1315/37/1/012064.

Basara, J.B., Basara, H.G., Illston, B.G. and Crawford, K.C. (2010). The impact of the urban heat islands during an intense heat wave in Oklahoma City. *Advanced Meteorological*

Chander, G. and Markham, B. (2003). Revised Landsat-5 TM radiometric calibration procedures and post calibration dynamic ranges. *IEEE Transactions on Geoscience and Remote Sensing*, 41, 2674–2677.

Chen, A.; Yao, X.A.; Sun, R.; Chen, L. (2014). Effect of urban green patterns on surface urban cool islands and its seasonal variations.*Urban For. Urban Green*. 13, 646–654.

Evans, J.P. (2011). Developing an improved soil moisture dataset by blending passive and active microwave satellite-based retrievals. *Hydrol. Earth Syst. Sci*., 15, 425–436,

Florides, G. A. and Christodoulides, P, (2009). Global warming and carbon dioxide through sciences. *Environment International*, 35, 390–401.

Giannini M. B., Belfiore O.R., Parente, C. and Santamaria, R. (2015). Land Surface Temperature from Landsat 5 TM images: comparison of different methods using airborne thermal data

Grimmond, C.S.B. and Oke, T.R. (1991). An evapotranspiration-interception model for urban areas. *Water Resour. Res*.1991,27, 1739–1755.

Hussain, A., Bhalla, P., Palria, S. (2014). Remote sensing-based analysis of the role of land use/land cover on surface temperature and temporal changes in temperature: A case study of Ajmer District, Rajasthan. *ISPRS-Int Arch Photogram, Remote Sens Spat Info Sci*., 1: 1447-1454.

Jibril, I.U. (2010). The Return of the Greens in Abuja, Nigeria's New Capital City. FIG Congress 2010. *Sustainable Planning and Urban Renewal Facing the Challenges – Building the Capacity.* Sydney, Australia.

Khan, I.A., Arsalan, M.H., Siddiqut, M.F., Kiran, N., and Ajaib, M. (2016). Short-term drought assessment in Pakistan and adjoining areas by remote sensing MODIS-NDVI Data: A potential consequence of climate change. *Pakistan Journal of Botany*, 48, 1887-1892.

Khandelwal, H. (2017). Infrared regulating smart windows Eindhoven: Technische Universiteit Eindhoven.

Lafortezza, R., Carrus, G., Sanesi, G. and Davies, C. (2009). Benefits and wellbeing perceived by people visiting green spaces in periods of heat stress. *Urban For. Urban Green.*, 8, 97–108.

Li, Y., Zhao, M., Mildrexler, D. J., Motesharrei, S., Mu, Q., Kalnay, E.,Wang, K., (2016). Potential and actual impacts of deforestation and afforestation on land surface temperature. *Journal of Geophysical Research*, 121(24), 14372–14386

Liu, Y.Y., Parinussa, R.M., Dorigo, W.A., De Jeu, Wagner, W., van Dijk, A.M. McCabe, M.F.,

Makinde. E.O. and Agbor, C.F. (2019). Geoinformatic assessment of urban heat island and land use/cover processes: a case study from Akure. *Environmental Earth Sciences*, (2019) 78:483

Mwirigi M'Ikiugu. M., Kinoshita, T., Tashiro, Y., Procedia (2012). Urban green space analysis and identification of its potential expansion areas. *Social and Behavioral Sciences,* 35 (2012) 449 – 458.

Nastaran Shishegar (2014). The impact of green areas on mitigating urban heat island effect. *The International Journal of Environmental Sustainability*, 9(1), 119-130.

Nikolaos G. Silleos, Thomas K. Alexandridis, Ioannis Z. Gitas & Konstantinos Perakis, (2006). Vegetation Indices: Advances Made in Biomass Estimation and Vegetation Monitoring in the Last 30 Years. Geocarto International, Vol. 21, No. 4, December 2006

Nowak, D.J. and Crane, D.E. (2002). Carbon storage and sequestration by urban trees in the USA. *Environmental Pollution*, 116(3): 381–389.

Pickett, S.T.A; Cadenasso, M.L; Grove, J.M, Nilon, C.H.; Pouyat, R.V.Zipperer, W.C.and Costanza, R. (2001). Urban ecological systems: linking terrestrial ecological,

Qin, Z., and Karnieli, A. (1999). Progress in the remote sensing of land surface temperature and ground emissivity using NOAAAVHRR data. *International Journal of Remote Sensing*, 20: 2367-2393.

Raheem, W.M. and Adeboyejo, A.T., (2016). Urban greening and city sustainability in Ibadan metropolis, Nigeria. *Ethiopian Journal of Environmental studies and management*, 9(3):287-302.

Rahman, M.A.; Armson, D.; Ennos, A.R. (2014). Effect of urbanization and climate change in the rooting zone on the growth and physiology of Pyrus calleryana. *Urban For. Urban Green,* 13, 325–335.

Rahman, M.A.; Moser, A.; Rötzer, T.; Pauleit, S. (2017). Within canopy temperature differences and cooling ability of Tilia cordata trees grown in urban conditions. *Build. Environ.*, 114, 118–128.

Riphah U. S. (2015). Global Warming: Causes, Effects and Solutions. *Durresamin Journal*. 1 (4). 8PP.

Schneider, F. (2012). The Shadow Economy and Work in the Shadow**.** *IZA Discussion Paper* No. 6423.

Stafoggia, M.; Schwartz, J.; Forastiere, F.; Perucci, C.A. (2008). Does temperature modify the association between air pollution and mortality? A multicity case-crossover analysis in Italy. *Am. Journal of Epidemiology*,167, 1476–1485.

Stow, D.A. and Chen, D., (2002). Sensitivity of multi-temporal NOAA-AVHRR data for detecting land cover changes. *Remote sensing Environment*, 80, 297-307.

Tang, J. W. and Y. Z. (2007). Spatio-temporal urban landscape change analysis using the Markov chain model and a modified genetic algorithm, *28*(15), 3255–3271.

United Nations (2014). World Urbanization Prospects. New York: United Nations.
Walton, J.T., Nowak, D.J., Greenfield, E.J (2008). Assessing urban forest canopy cover. *Journal of Arboriculture and Urban Forestry* 34(6).
Weart, S. (2021). The discovery of global warming". *http://www.aip.org/history/climate*. 28PP.
Wilcox, R.I., Tom, A.A. and Akadi, A.P (2017). Impacts of Urban Expansion on Natural Vegetation in Uyo Metropolis. *International Journal of Social Sciences*, 11(3), 71-82.
Xiang, N. and Han, X. J (1997). Definition and Contents of spatial analysis, central south University of Technology, 4: 28. https://doi.org/10.1007/s11771-997-0025-0
Yilmaz, S.; Toy, S.; Irmak, M.A.; Yilmaz, H. (2007). Determination of climatic differences in three different land uses in the city of Erzurum, Turkey. *Build. Environ*.,42, 1604–1612.
Zhou W., Cao F. and Wang G. (2019). Effects of spatial pattern of forest vegetation on urban cooling in a compact megacity. *Forests*, 10, 282.